J|A|C|S
ARTICLES
Published on Web 02/05/2008

Efficient Exciton Transport in Layers of Self-Assembled Porphyrin Derivatives

Annemarie Huijser,*,† Bart M. J. M. Suijkerbuijk,‡ Robertus J. M. Klein Gebbink,‡ Tom J. Savenije,† and Laurens D.A. Siebbeles†

Opto-Electronic Materials Section, DelftChemTech, Delft University of Technology, Julianalaan 136, 2628 BL Delft, The Netherlands, and Chemical Biology and Organic Chemistry, Faculty of Science, Utrecht University, Padualaan 8, 3584 CH Utrecht, The Netherlands

Received July 11, 2007; E-mail: L.D.A. Siebbeles@tudelft.nl

Abstract: The photosynthetic apparatus of green sulfur bacteria, the chlorosome, is generally considered as a highly efficient natural light-harvesting system. The efficient exciton transport through chlorosomes toward the reaction centers originates from self-assembly of the bacteriochlorophyll molecules. The aim of the present work is to realize a long exciton diffusion length in an artificial light-harvesting system using the concept of self-assembled natural chlorosomal chromophores. The ability to transport excitons is studied for porphyrin derivatives with different tendencies to form molecular stacks by self-assembly. A porphyrin derivative denoted as ZnOP, containing methoxymethyl substituents ({*meso*-tetrakis[3,5-bis(methoxymethyl)-phenyl]porphyrinato}zinc(II)) is found to form self-assembled stacks, in contrast to a derivative with *tert*-butyl substituents, ZnBuP ({*meso*-tetrakis[3,5-bis(*tert*-butyl)phenyl]porphyrinato}zinc(II)). Exciton transport and dissociation in a bilayer of these porphyrin derivatives and TiO_2 are studied using the time-resolved microwave conductivity (TRMC) method. For ZnOP layers it is found that excitons undergo diffusive motion between the self-assembled stacks, with the exciton diffusion length being as long as 15 ± 1 nm, which is comparable to that in natural chlorosomes. For ZnBuP a considerably shorter exciton diffusion length of 3 ± 1 nm is found. Combining these exciton diffusion lengths with exciton lifetimes of 160 ps for ZnOP and 74 ps for ZnBuP yields exciton diffusion coefficients equal to 1.4×10^{-6} m^2/s and 1×10^{-7} m^2/s, respectively. The larger exciton diffusion coefficient for ZnOP originates from a strong excitonic coupling for interstack energy transfer. The findings show that energy transfer is strongly affected by the molecular organization. The efficient interstack energy transfer shows promising prospects for application of such self-assembled porphyrins in optoelectronics.

Introduction

The occurrence of photosynthesis is crucial for life on earth. The first essential step in photosynthesis is the capture of sunlight. To absorb sunlight efficiently, photosynthetic organisms are equipped with light-harvesting systems. These light-harvesting systems are typically based on ring-like bacteriochlorophyll−protein complexes. The proteins determine the three-dimensional structure of the light-harvesting complex. The main function of the bacteriochlorophyll molecules involves the absorption of sunlight. Absorption of a photon results in the formation of a strongly bound electron−hole pair, also referred to as an exciton. Due to the specific mutual orientation of adjacent bacteriochlorophyll molecules, excitons are transported efficiently through one or more light-harvesting complexes over distances of typically 10−20 nm toward the reaction center, where exciton dissociation into charged species takes place.[1−8]

An alternative efficient exciton transport pathway can, however, also be present in systems that lack a protein matrix; an example is the chlorosome, the photosynthetic system in green photosynthetic bacteria. The chlorosome is an ellipsoidal shaped organelle with a typical size of 15 nm × 30 nm × 100 nm,[9] based on self-assembled bacteriochlorophyll *c*, *d*, or *e* molecules organized by bacteriochlorophyll−bacteriochlorophyll rather than by bacteriochlorophyll−protein interactions.[10−13]

† Delft University of Technology.
‡ Utrecht University.

(1) Amerongen, H. v.; Valkunas, L.; Grondelle, R. v. *Photosynthetic excitons*; World Scientific: Singapore, 2000.
(2) Kühlbrandt, W.; Wang, D. N. *Nature* **1991**, *350*, 130−134.
(3) Krauss, N.; Hinrichs, W.; Witt, I.; Fromme, P.; Pritzkow, W.; Dauter, Z.; Betzel, C.; Wilson, K. S.; Witt, H. T.; Saenger, W. *Nature* **1993**, *361* (6410), 326−331.
(4) Kühlbrandt, W.; Neng Wang, D.; Fujiyoshi, Y. *Nature* **1994**, *367*, 614−621.
(5) McDermott, G.; Prince, S. M.; Freer, A. A.; Hawthornwaite-Lawless, A. M.; Papiz, M. Z.; Cogdell, R. J.; Isaacs, N. W. *Nature* **1995**, *374*, 517−521.
(6) Oijen, A. M. v.; Ketelaars, M.; Köhler, J.; Aartsma, T. J.; Schmidt, J. *Science* **1999**, *285*, 400−402.
(7) Roszak, A. W.; Howard, T. D.; Southall, J.; Gardiner, A. T.; Law, C. J.; Isaacs, N. W.; Cogdell, R. W. *Science* **2003**, *302*, 1969−1972.
(8) Liu, Z.; Yan, H.; Wang, K.; Kuang, T.; Zhang, J.; Gui, L.; An, X.; Chang, W. *Nature* **2004**, *428*, 287−292.
(9) Staehelin, L. A.; Golecki, J. R.; Fuller, R. C.; Drews, G. *Arch. Microbiol.* **1978**, *119*(3), 269−277.
(10) Holzwarth, A. R.; Griebenow, K.; Schaffner, K. *Z. Naturforsch.* **1990**, *45* (3−4), 203−206.
(11) Hildebrandt, P.; Griebenow, K.; Holzwarth, A. R.; Schaffner, K. *Z. Naturforsch.* **1991**, *46* (3−4), 228−232.
(12) Psencik, J.; Ikonen, T. P.; Laurinmaki, P.; Merckel, M. C.; Butcher, S. J.; Serimaa, R. E.; Tuma, R. *Biophys. J.* **2004**, *87* (2), 1165−1172.
(13) Balaban, T. S.; Holzwarth, A. R.; Schaffner, K.; Boender, G. J.; Degroot, H. J. M. *Biochemistry* **1995**, *34* (46), 15259−15266.

Essential for self-assembly of the bacteriochlorophyll molecules in the chlorosome are (a) the coordinative bonds between electron-donating side groups and the electron-accepting Mg center of the molecule and (b) the $\pi-\pi$ interactions between the bacteriochlorophyll macrocycles.[10,11,14−18] Excitons are transferred through the self-assembled stacks over distances of typically 10−15 nm[12] to a bacteriochlorophyll *a* containing base plate, connected to the chlorosomal vesicle, and further toward a reaction center. Energy transfer between adjacent bacteriochlorophyll molecules within one self-assembled stack occurs extremely rapidly, typically on a time scale of 100 fs, corresponding to an energy transfer rate (k_{ET}) equal to 10^{13} s^{-1}.[19−21] If we assume an exciton to be localized on one bacteriochlorophyll molecule, the exciton diffusion coefficient (D_E) follows from

$$D_E = k_{ET} R_{DA}{}^2 \quad (1)$$

where R_{DA} presents the center-to-center distance between adjacent bacteriochlorophyll molecules. Combination of the exciton diffusion coefficient with the exciton lifetime (τ_E) yields the exciton diffusion length (Λ_E), according to

$$\Lambda_E = \sqrt{D_E \tau_E} \quad (2)$$

The center-to-center distance of 6.8 Å[22] and the energy transfer rate of typically 10^{13} s^{-1} result in an exciton diffusion coefficient of about 5×10^{-6} m^2/s. Hence, during the lifetime of typically 50 ps[19] an exciton can make on average 5×10^2 hops, and Λ_E is on the order of 15 nm. This length is close to the average distance between the location of exciton formation and the bacteriochlorophyll *a* containing base plate,[9] so that almost all photogenerated excitons arrive at the reaction center.

In contrast to natural systems, Λ_E in molecular organic dye layers is typically on the order of only a few nanometers.[23−25] For a few molecular dye systems, exciton diffusion lengths of several tens of nanometers have been realized in vacuum thermal deposited layers.[26−29] The expensive and elaborate deposition method makes these layers, however, less attractive for application in molecular devices. In this context, porphyrin derivatives are of great interest, since thin films of this class of materials can be prepared by spincoating. For several free-base and zinc *meso*-tetrakisphenylporphyrin derivatives, the introduction of appropriate alkyl substituents has been reported to affect the molecular organization and consequently the exciton diffusion length.[30−33] The introduction of octyl side chains has been observed to result in the formation of molecular stacks along which excitons can undergo intrastack diffusion with $\Lambda_E = 9 \pm 3$ nm.[31] In contrast, exciton diffusion between stacks has been found to be considerably less efficient.[30,31] The latter is problematic, since for optoelectronic applications efficient exciton transport through the organic layer toward an active (e.g., electron-accepting) interface has to be directed perpendicular to this interface, while the molecular stacks tend to align parallel to a substrate.[30,34] Recently, we have reported a lower limit for Λ_E in the direction perpendicular to a TiO_2 substrate of 12 nm for a system based on nematically organized, homeotropically aligned *meso*-tetrakis(4-*n*-butylphenyl)porphyrin molecules.[35] However, the favorable molecular organization has only been obtained for layers thinner than 35 nm, which can be an important limitation for application in practical devices.

The aim of the current study is to achieve efficient energy transfer toward an active interface using the concept of self-assembled chromophore molecules. Numerous reports deal with the synthesis and structural characterization of self-assembling mimics of bacteriochlorophyll molecules, such as the robust and relatively easily available porphyrin and chlorin derivatives.[36−45] So far, no experimental demonstration of long-range exciton diffusion for such systems has been published. In this work the relationship between self-assembly and the ability to transport excitons is studied for two porphyrin derivatives, namely {*meso*-tetrakis[3,5-bis(dimethylaminomethyl)phenyl]porphyrinato}zinc-(II) (ZnNP) and {*meso*-tetrakis[3,5-bis(methoxymethyl)phenyl]-porphyrinato}zinc(II) (ZnOP). The chemical structures of these porphyrin derivatives are shown in Figure 1A. Self-assembly is accomplished by the formation of coordinative bonds between the electron-accepting Zn atom and the electron-donating benzylic heteroatoms at the 3- or the 5-position of the *meso*-phenyl rings of an adjacent molecule. A close analogue of ZnOP having Br atoms at the para-positions of the phenyl groups (ZnOPBr) has recently been observed by single-crystal X-ray crystallography to self-assemble as shown in Figure 1B.[46] Since ZnNP and especially ZnOP possess equivalent electron-donating

(14) Rossum, B. J. v.; Steengaard, D. B.; Mulder, F. M.; Boender, G. J.; Schaffner, K.; Holzwarth, A. R.; Groot, H. J. M. d. *Biochemistry* **2001**, *40*, 1587−1595.
(15) Balaban, T. S.; Linke-Schaetzel, M., et al. *Chem.−Eur. J.* **2005**, *11* (8), 2267−2275.
(16) Overmann, J.; Cypionka, H.; Pfennig, N. *Limnol. Oceanogr.* **1992**, *37*, 150−155.
(17) Frigaard, N. U.; Chew, A. G. M.; Li, H.; Maresca, J. A.; Bryant, D. A. *Photosynth. Res.* **2003**, *78*(2), 93−117.
(18) Frigaard, N. U.; Bryant, D. A. *Arch. Microbiol.* **2004**, *182*, 265−276.
(19) Prokhorenko, V. I.; Steensgaard, D. B.; Holzwarth, A. F. *Biophys. J.* **2000**, *79* (4), 2105−2120.
(20) Psencik, J.; Polivka, T.; Nemec, P.; Dian, J.; Kudrna, J.; Maly, P.; Hala, J. *J. Phys. Chem. A* **1998**, *102* (23), 4392−4398.
(21) Savikhin, S.; Zhu, Y. W.; Lin, S.; Blankenship, R. E.; Struve, W. S. *J. Phys. Chem.* **1994**, *98* (40), 10322−10334.
(22) Holzwarth, A. R.; Schaffner, K. *Photosynth. Res.* **1994**, *41*, 225−233.
(23) Wohrle, D.; Tennigkeit, B.; Elbe, J.; Kreienhoop, L.; Schnurpfeil, G. *Mol. Cryst. Liq. Cryst.* **1993**, *230*, 221−226.
(24) Kerp, H. R.; Donker, H.; Koehorst, R. B. M.; Schaafsma, T. J.; Faassen, E. E. v. *Chem. Phys. Lett.* **1998**, *298*(4−6), 302−308.
(25) Kroeze, J. E.; Savenije, T. J.; Warman, J. M. *J. Photochem. Photobiol. A* **2002**, *148*, 49−55.
(26) Peumans, P.; Uchida, S.; Forrest, S. R. *Nature* **2003**, *425* (6954), 158−162.
(27) Peumans, P.; Forrest, S. R. *Appl. Phys. Lett.* **2001**, *79* (1), 126−128.
(28) Peumans, P.; Yakimov, A.; Forrest, S. R. *J. Appl. Phys.* **2003**, *93* (7), 3693−3723.
(29) Stubinger, T.; Brutting, W. *J. Appl. Phys.* **2001**, *90* (7), 3632−3641.
(30) Kroeze, J. E.; Koehorst, R. B. M.; Savenije, T. J. *Adv. Funct. Mater.* **2004**, *14* (10), 992−998.
(31) Donker, H.; van Hoek, A.; van Schaik, W.; Koehorst, R. B. M.; Yatskou, M. M.; Schaafsma, T. J. *J. Phys. Chem. B* **2005**, *109* (36), 17038−17046.
(32) Huijser, A.; Savenije, T. J.; Kroeze, J. E.; Siebbeles, L. D. A. *J. Phys. Chem. B* **2005**, *109*, 20166−20173.
(33) Huijser, A.; Savenije, T. J.; Siebbeles, L. D. A. *Thin Solid Films* **2006**, *511−512*, 208−213.
(34) Piris, J.; Debije, M. G.; Stutzmann, N.; van de Craats, A. M.; Watson, M. D.; Mullen, K.; Warman, J. M. *Adv. Mater.* **2003**, *15* (20), 1736−1740.
(35) Huijser, A.; Savenije, T. J.; Kotlewski, A.; Picken, S. J.; Siebbeles, L. D. A. *Adv. Mater.* **2006**, *18*, 2234−2239.
(36) Jesorka, A.; Balaban, T. S.; Holzwarth, A. R.; Schaffner, K. *Angew. Chem., Int. Ed.* **1996**, *23−24*, 2861−2863.
(37) Tamiaki, H. *Coord. Chem. Rev.* **1996**, *148*, 183−197.
(38) Miyatake, T.; Tamiaki, H.; Holzwarth, A. R.; Schaffner, K. *Helv. Chim. Acta* **1999**, *82* (6), 797−810.
(39) Balaban, T. S.; Goddard, R.; Linke-Schaetzel, M.; Lehn, J. M. *J. Am. Chem. Soc.* **2003**, *125* (14), 4233−4239.
(40) Balaban, T. S. *Acc. Chem. Res.* **2005**, *38* (8), 612−623.
(41) Kunieda, M.; Tamiaki, H. *J. Org. Chem.* **2005**, (70), 820−828.
(42) Kunieda, M.; Tamiaki, H. *Eur. J. Org. Chem.* **2006**, *10*, 2352−2361.
(43) Huber, V.; Lysetska, M.; Wurthner, F. *Small* **2007**, *3* (6), 1007−1014.
(44) Zhou, Y. S.; Wang, B.; Zhu, M. Z.; Hou, J. G. *Chem. Phys. Lett.* **2005**, *403* (1−3), 140−145.
(45) Elemans, J.; Lensen, M. C.; Gerritsen, J. W.; van Kempen, H.; Speller, S.; Nolte, R. J. M.; Rowan, A. E. *Adv. Mater.* **2003**, *15* (24), 2070−2073.

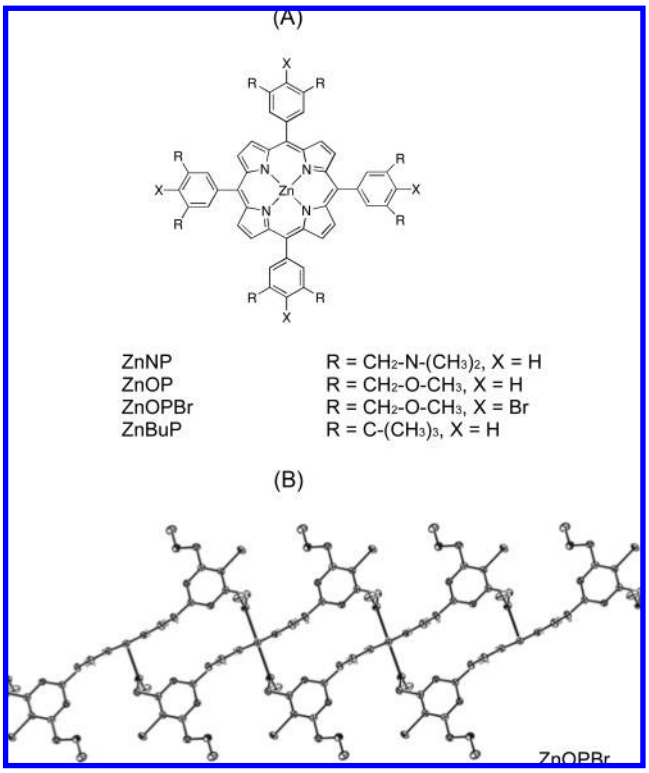

Figure 1. Chemical structures of the porphyrin derivatives investigated (A) and a part of the one-dimensional self-assembled stack formed by ZnOPBr molecules (B). Hydrogen atoms and phenyl side groups that are not involved in the self-assembly are omitted for clarity.

and electron-accepting groups, comparable self-assembling behavior is expected, as also proposed earlier[46] and validated below. ZnOPBr is not included in the current study on exciton transfer, since the heavy Br atom leads to significant intersystem crossing from singlet to triplet excited states,[47] which will be the topic of another study. To substantiate the impact of self-assembly on the exciton diffusion length, also a porphyrin derivative that is expected not to self-assemble is studied, namely {*meso*-tetrakis[3,5-bis(*tert*-butyl)phenyl]porphyrinato}zinc(II) (ZnBuP). The benzylic substituents of ZnBuP possess a similar steric bulk to that of the CH_2OCH_3 and $CH_2N(CH_3)_2$ groups but lack the electron-donating ability.

The molecular organization in spincoated films of the porphyrin derivatives investigated is studied using optical techniques and X-ray diffraction. Exciton transport and dissociation in a bilayer of the porphyrin derivatives and smooth TiO_2 are studied using the time-resolved microwave conductivity (TRMC) method. Excitons are formed by illumination with a nanosecond laser pulse. Those excitons that are able to reach the interface with TiO_2 can undergo interfacial dissociation into separate charge carriers. The electrons injected into the TiO_2 layer are monitored by measuring the microwave conductivity. The exciton diffusion length and the interfacial electron injection yield are determined from fitting an analytical model to the experimental microwave conductivity data. The energy transfer rate between adjacent molecules is strongly affected by molecular self-assembly. This offers promising prospects for use of these materials to convert solar energy into chemical or electrical energy in, e.g., photocatalytic applications, sensors, and photovoltaics.[48−51]

Experimental Section

Synthesis of Porphyrin Derivatives. The porphyrin derivatives ZnOP, ZnNP, and ZnBuP were synthesized as described in ref 46.

Sample Preparation. Thin smooth anatase TiO_2 films with a thickness of ca. 100 nm, prepared by chemical vapor deposition onto $1 \times 12 \times 25$ mm^3 quartz substrates, were purchased from Everest Coatings, Delft, The Netherlands. Porphyrin films were prepared by spincoating, either from a solution in $CHCl_3$ (Anhydrous, 99+%, Aldrich, in case of ZnOP, ZnOPBr and ZnBuP) or from a solution in toluene (Anhydrous, 99.8%, Aldrich, used for ZnNP) at 2500 rpm under N_2 atmosphere. The ZnNP solution was filtrated using a 0.45 μm PTFE filter with polypropylene housing. Prior to film deposition, the quartz and TiO_2 substrates were annealed in air at 450 °C for 1 h. After porphyrin film deposition, the samples were annealed at 200 °C under a N_2 atmosphere for 15 min. Porphyrin film thicknesses were determined using a Veeco Dektak 8 Stylus Profiler.

Optical Characterization. Optical transmission and reflection spectra were recorded using a Perkin-Elmer Lambda 900 UV/vis/NIR spectrometer. The optical density (*OD*), the fraction of absorbed light (F_A), and the extinction coefficient (ϵ) were determined as described in ref 52. The wavelength dependent *OD* and F_A are denoted as the absorption spectrum and the optical attenuation spectrum, respectively. Steady-state and time-resolved fluorescence spectra were recorded with a Lifespec − ps setup using a 405 nm excitation source (Edinburgh Instruments). Polarized Optical micrographs of the porphyrin films were recorded between crossed polarizers using a Nikon Eclipse E600 Polarizing Optical Microscope.

X-ray Diffraction Analysis. X-ray diffraction (XRD) measurements were performed in the Bragg−Brentano mode on a Bruker-AXS D8 Advance powder X-ray diffractometer, equipped with automatic divergence slits and a Våntec-1 detector and using a Co anode ($\lambda_{K\alpha}$ = 1.790 26 Å) operated at 30 kV and 45 mA. The X-ray diffraction intensity found for a bare substrate was subtracted from the intensity observed for a porphyrin-coated substrate.

Photoconductivity Experiments. The TRMC method and experimental setup are described in refs 25 and 53. The porphyrin/TiO_2 bilayers were mounted in an X-band microwave cavity at a position of maximum electric field strength and illuminated either from the side of the TiO_2 substrate (backside) or from the side of the porphyrin film (front side). The illumination intensity was varied between 10^{11} and 10^{13} photons/cm^2 per pulse. The data analysis has been described in detail previously.[52,53] Briefly, formation of mobile charge carriers due to illumination with a nanosecond laser pulse (3 ns fwhm) leads to an increase of the photoconductance (ΔG), followed by an eventual decrease due to decay of charge carriers. The increase in photoconductance is related to the normalized change in reflected microwave power ($\Delta P/P$) according to

$$\frac{\Delta P(t)}{P} = -K\Delta G(t) \qquad (3)$$

The sensitivity factor K was determined as described in ref 54 and equals 7×10^4 S^{-1}. From the maximum of ΔG during time, the incident

(46) Suijkerbuijk, B. M. J. M.; Tooke, D. M.; Lutz, M.; Spek, A. L.; Koten, G. v.; Klein Gebbink, R. J. M. *Chem. Asian J.* **2007**, *2*, 889−903.
(47) Gouterman, M. *The Porphyrins, Volume III*. Academic Press: New York, 1978; Vol. 3.
(48) Gerdes, R.; Wohrle, D.; Spiller, W.; Schneider, G.; Schnurpfeil, G.; Schulz-Ekloff, G. *J. Photochem. Photobiol. A* **1997**, *111* (1−3), 65−74.
(49) Iliev, V.; Mihaylova, A.; Bilyarska, L. *J. Mol. Catal. A* **2002**, *184* (1−2), 121−130.
(50) Grätzel, M. *Nature* **2001**, *414*, 338−344.
(51) Gust, D.; Moore, T. A.; Moore, A. L. *Acc. Chem. Res.* **2001**, *34*, 40−48.
(52) Kroeze, J. E.; Savenije, T. J.; Warman, J. M. *J. Am. Chem. Soc.* **2004**, *126*, 7608.
(53) Haas, M. P. d.; Warman, J. M. *Chem. Phys.* **1982**, *73*, 35−53.
(54) Savenije, T. J.; Haas, M. P. d.; Warman, J. M. *Zeitschrift fur Physikalische Chemie-International Journal of Research in Physical Chemistry & Chemical Physics* **1999**, *212*, 201−206.

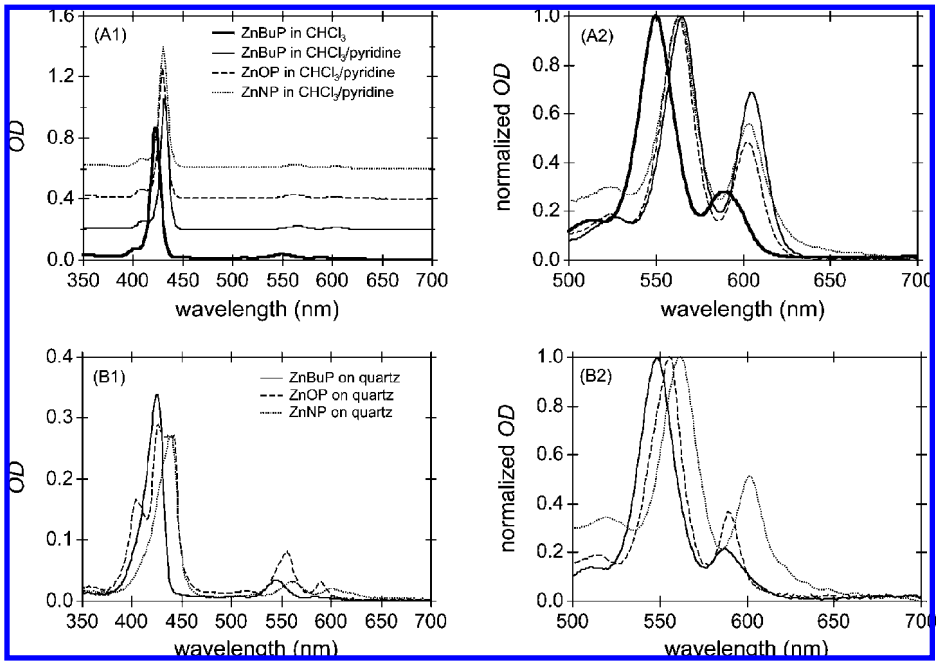

Figure 2. Optical density spectra of the porphyrin derivatives in solution (A) and deposited on quartz (B). The data in Figure A1 have different offsets. Left panels show the full *OD* spectrum; right panels show the normalized *OD* for a limited spectral region.

photon to charge separation efficiency (*IPCSE*) was determined, as described in ref 32.

Results and Discussion

Structural Characterization. In case the formation of a coordinative bond between the electron-accepting central Zn atom and an electron-donating side group of an adjacent molecule leads to a change in optical features, the occurrence of self-assembly can be determined using optical absorption and fluorescence spectroscopy.[39,55,56] Figure 2A shows the absorption spectrum of ZnBuP monomers dissolved in pure $CHCl_3$, which is found to be similar to the absorption spectra of ZnOP and ZnNP in pure $CHCl_3$. The transitions from the S_0 to the S_1 level and a higher vibrational mode give rise to the two Q-bands that peak at 589 and 550 nm, respectively. The S_0-S_2 transition results in a strong absorption band that peaks at 423 nm.[47] The data in Figure 2A show that addition of 25 μL of pyridine leads to a red-shift of the absorption bands (peaks at 605, 565, and 431 nm) and a more intense lowest Q-band. These changes in optical features are attributed to the formation of one-to-one complexes of pyridine with the ZnBuP molecule, resulting in a penta-coordination of the Zn atom.[57,58] The absorption spectra of ZnOP and ZnNP in $CHCl_3$/pyridine are observed to be similar to that of ZnBuP in $CHCl_3$/pyridine. Hence, the difference in benzylic substituents does not affect the absorption spectra.

Analogous to the changes in monomer absorption due to coordination of the central Zn atom by pyridine, molecular self-assembly in solid films can be monitored by a red-shift in absorption and a more intense lowest Q-band.[57] Figure 2B shows the absorption spectra of ZnBuP, ZnOP, and ZnNP deposited on quartz. The absorption bands of ZnBuP on quartz are only broadened as compared to ZnBuP dissolved in $CHCl_3$. The absence of a red-shift and a more intense lowest Q-band in the absorption spectrum shows that most likely no coordinative bonds are present in the film, indicative of the absence of self-assembled ZnBuP molecules. In contrast, the absorption spectra of ZnOP and especially ZnNP on quartz show a considerable red-shift and a more intense lowest Q-band as compared to ZnBuP. This is attributed to the presence of coordinative bonds between the electron-accepting Zn atom and the electron-donating oxygen or nitrogen atoms in the side groups. The red-shift in absorption and increase of the intensity of the lowest Q-band are less pronounced for ZnOP than those for ZnNP, which might originate from the stronger coordinative bond in the case of the latter.[46,59] The Soret absorption band of the ZnOP film shows a more pronounced split than that for ZnNP. This is attributed to a stronger excitonic coupling between self-assembled ZnOP molecules in a stack, possibly caused by a smaller center-to-center distance between adjacent molecules[46] leading to a larger excitonic splitting. In terms of the point−dipole approximation for the excitonic coupling,[60] the absence of a significant exciton splitting in the less intense Q-bands can be attributed to the lower transition dipole moments of the corresponding transitions as compared to the S_0-S_2 transition that gives rise to the Soret absorption band.

Figure 3A shows the fluorescence spectra for ZnBuP, ZnOP, and ZnNP on quartz. In agreement with the results discussed above, ZnOP and especially ZnNP exhibit red-shifted fluorescence bands as compared to ZnBuP, indicative of molecular self-assembly of the first two. Figure 3B shows the fluorescence decays of the ZnBuP, ZnOP, and ZnNP films on quartz. Fitting a monoexponential function convoluted with the instrumental response function to the decays yields exciton lifetimes of 74,

(55) Chernook, A. V.; Rempel, U.; vonBorczyskowski, C.; Shulga, A. M.; Zenkevich, E. I. *Chem. Phys. Lett.* **1996**, *254* (3−4), 229−241.
(56) Lee, S. J.; Mulfort, K. L.; O'Donnell, J. L.; Zuo, X. B.; Goshe, A. J.; Wesson, P. J.; Nguyen, S. T.; Hupp, J. T.; Tiede, D. M. *Chem. Commun.* **2006**, (44), 4581−4583.
(57) Fleischer, E. B.; Shachter, A. M. *Inorg. Chem.* **1991**, *30* (19), 3763−3769.
(58) Summers, J. S.; Stolzenberg, A. M. *J. Am. Chem. Soc.* **1993**, *115* (23), 10559−10567.
(59) Nardo, J. V.; Dawson, J. H. *Inorg. Chim. Acta* **1986**, *123* (1), 9−13.
(60) May, V.; Kühn, O. *Charge and Energy Transfer Dynamics in Molecular Systems. A Theoretical Introduction*; Wiley-VCH: Berlin, 2000.

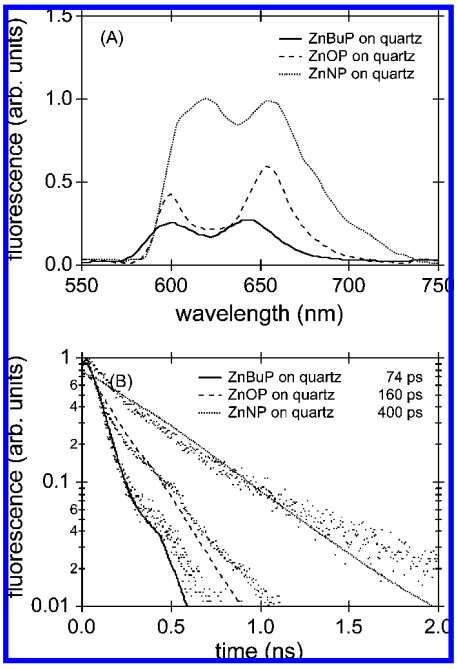

Figure 3. Fluorescence spectra (A) and decays (B) of the porphyrin derivatives investigated on quartz, recorded on excitation at 405 nm. The fluorescence decays are detected at the maximum of the lowest fluorescence band. Fits of a monoexponential function convoluted with the instrumental response function to the fluorescence decays and the resulting lifetimes are included.

160, and 400 ps. The fits are included in Figure 3B. These lifetimes are significantly lower than the 1.3 ns lifetime observed for these porphyrin derivatives dissolved in $CHCl_3$/pyridine (data not shown), which is most likely due to enhanced radiationless decay in solid films.

The differences in optical features between ZnBuP films on one side and the ZnOP and ZnNP films on the other side are attributed to the presence of coordinative bonds for the latter two, indicative of molecular self-assembly. To obtain further insight in the molecular organization, polarized optical microscopy (POM) and X-ray diffraction (XRD) studies are performed. Figure 4A shows the polarized optical micrograph and the X-ray diffraction pattern of ZnBuP on quartz. The ZnBuP film appears dark between crossed polarizer and analyzer and remains dark on rotation of the sample around the axis perpendicular to the plane of the film. This implies that the polarization of the incident light beam does not change upon transmission through the ZnBuP film. As a consequence, the transmitted light cannot pass through the crossed analyzer, resulting in a dark appearance of the film. The observed findings indicate an isotropic film structure with respect to rotation around the axis perpendicular to the plane of the film. This could be either due to an isotropic layer structure or due to a homeotropic molecular alignment (molecular planes aligned parallel to the substrate). The absence of a diffraction peak in the XRD pattern excludes the latter possibility and leads to the conclusion that the ZnBuP film lacks any molecular organization.

The X-ray diffraction pattern of ZnOPBr deposited on quartz, shown in Figure 4B, differs significantly from that of ZnBuP on quartz. The pronounced peaks in the XRD pattern observed for ZnOPBr originate from a well-developed periodic structure directed perpendicular to the substrate. The two peaks observed can be explained by first- and second-order diffraction by parallel planes with an interplanar distance (d) equal to 14.8 Å. This distance agrees with the diameter of a self-assembled stack of about 15 Å or, equivalently, with the distance between adjacent self-assembled stacks. Since only a periodic structure directed perpendicular to the substrate can give rise to a diffraction peak, this would imply the alignment of the propagation direction of the self-assembled stacks parallel to the substrate. In previous work on ZnOPBr crystals, the center-to-center distance R_{DA} between ZnOPBr molecules within a self-assembled stack has been found to be 8.75 Å, while the distance between the ZnOPBr macrocycles equals only 3.47 Å.[46] In case the ZnOPBr molecules in a crystal and in a thin film self-assemble in a similar way and the propagation direction of the self-assembled stacks in a film is parallel to the substrate, the angle between the ZnOPBr macrocycles and the substrate equals 23° as shown schematically in Figure 4.

The polarized optical micrograph and XRD pattern of ZnOP on quartz, also shown in Figure 4B, are observed to be similar to those for ZnOPBr. The first- and second-order X-ray diffraction peaks are only slightly shifted toward higher angles. These peaks correspond to an interplanar distance equal to 14.01 Å. The slightly smaller interplanar distance as compared to ZnOPBr and less intense diffraction peaks are attributed to the absence of the Br atoms. Both ZnOPBr and ZnOP exhibit similar birefringent domains between crossed polarizer and analyzer. The birefringence is caused by an anisotropy of the index of refraction, leading to a splitting of the linearly polarized incident beam into two components with polarizations perpendicular to each other. As a consequence, part of the transmitted light beam can pass through the crossed analyzer, leading to a bright appearance of the film. The observed birefringence independently confirms the presence of molecular order in the ZnOPBr and ZnOP films. The birefringence is observed to be comparable for layers deposited on TiO_2 and quartz, as also observed previously,[35] showing a similar molecular organization on both substrates. The ordered domains have a typical area of 10 μm $\times$ 10 μm and a thickness of 50 nm. The comparable X-ray diffraction patterns and polarized optical micrographs suggest similar mutual orientations for the individual molecules in a self-assembled stack and for the alignment of the stacks with respect to the substrate. This implies that the propagation direction of the self-assembled ZnOP stacks is parallel to the substrate, with the angle between the ZnOP macrocycles and the substrate equal to 23°.

Figure 4C shows the polarized optical micrograph and the X-ray diffraction pattern of ZnNP on quartz. The ZnNP film appears to possess both dark and birefringent domains between crossed polarizer and analyzer, corresponding to a combination of disordered and ordered regions, respectively. The X-ray diffraction peak observed for the ZnNP film corresponds in case of first-order diffraction to an interplanar distance equal to 16.6 Å, which is attributed to the distance between adjacent self-assembled stacks. The fact that only the ordered domains can contribute to the observed diffraction peak explains the lower intensity of this peak as compared to that observed for the ZnOP film.

Determination of the Exciton Diffusion Length. Quantification of the exciton transfer dynamics allows determining the impact of molecular order on the ability to transport excitons efficiently. Exciton diffusion is studied using the time-resolved

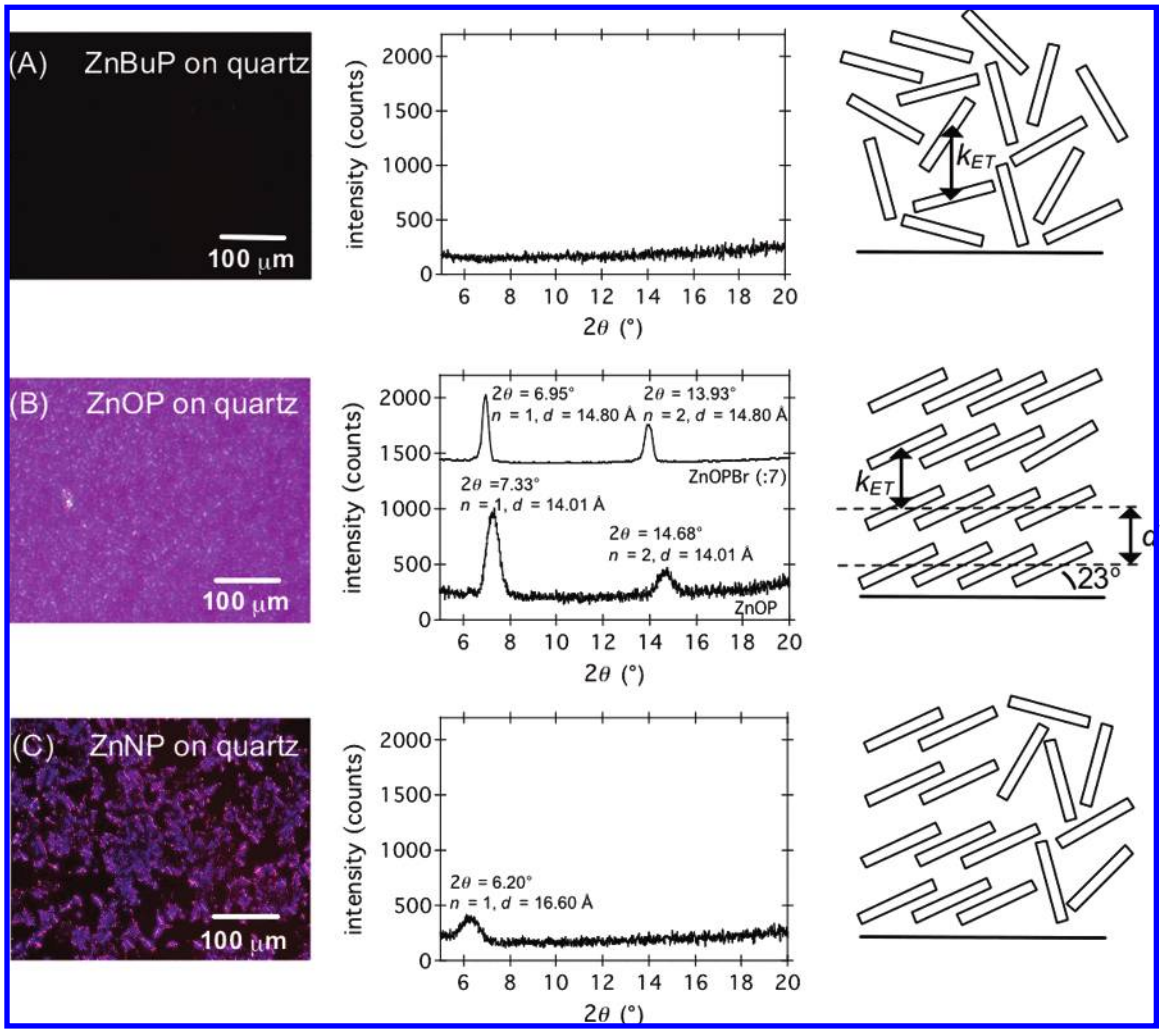

Figure 4. Polarized optical micrographs obtained between crossed polarizer and analyzer (left panels), X-ray diffraction patterns (middle panels), and film structures (right panels) of the porphyrin derivatives investigated on quartz. The X-ray diffraction intensities of the porphyrin films on quartz are corrected for the signal obtained for bare quartz.

microwave conductivity (TRMC) technique.[25,53] Figure 5A shows the photoconductance transients obtained on pulsed illumination at the absorption maximum of ZnBuP, ZnOP, and ZnNP films on TiO_2. The samples are illuminated through the TiO_2 layer, resulting in a high initial exciton concentration near the TiO_2/porphyrin interface. Those excitons that are able to reach the interface with TiO_2 can dissociate by injection of an electron into the TiO_2 layer. Since the mobility of electrons in TiO_2[61] largely exceeds the mobility of holes in porphyrins,[62] the observed change in photoconductance (ΔG) mainly results from an increase of the number of mobile electrons in TiO_2. The initial rise time of ΔG largely exceeds the laser pulse duration and is determined by the 18 ns response time of the microwave cavity. It follows from Figure 5A that illumination of a bilayer consisting of the self-assembled porphyrin derivatives ZnOP or ZnNP on TiO_2 results in a larger change in ΔG as compared to a bilayer of nonassembled ZnBuP and TiO_2. This effect is most pronounced for ZnOP on TiO_2, indicative of the most efficient photoinduced charge separation.

The incident photon to charge separation efficiency (*IPCSE*) is determined from ΔG as described in ref 32. Figure 5B shows the *IPCSE* as function of wavelength of ZnOP on TiO_2. The *IPCSE* spectrum follows closely the optical attenuation spectrum, also presented in Figure 5B, which demonstrates clearly photosensitization of TiO_2 by the porphyrin derivative. The *IPCSE* at the absorption maximum equals 16%, comparable to the efficiency of the system based on nematically organized homeotropically aligned *meso*-tetrakis(4-*n*-butylphenyl)porphyrin molecules on TiO_2 we have studied recently.[35] An important advantage of ZnOP as compared to that system involves the absence of any observed sensitivity of the molecular organization to the thickness of the porphyrin layer, which is highly beneficial for application in molecular optoelectronics. Figure 5C shows the *IPCSE* as a function of incident light intensity. At illumination intensities below 2×10^{12} photons/cm^2/pulse no significant influence of the intensity on the *IPCSE* is observed. This indicates that exciton−exciton annihilation and bimolecular charge recombination processes are insignificant under these illumination conditions.

The exciton diffusion length (Λ_E) can be deduced by applying an analytical model for the photoinduced charge separation efficiency to describe the experimental TRMC data, as discussed

(61) Bak, T.; Nowotny, J.; Rekas, M.; Sorrell, C. C. *J. Phys. Chem. Solids* **2003**, *64* (7), 1069−1087.
(62) Checcoli, P.; Conte, G.; Salvatori, S.; Paolesse, R.; Bolognesi, A.; Berliocchi, A.; Brunetti, F.; D'Amico, A.; Di Carlo, A.; Lugli, P. t. *Synth. Met.* **2003**, *138* (1−2), 261−266.

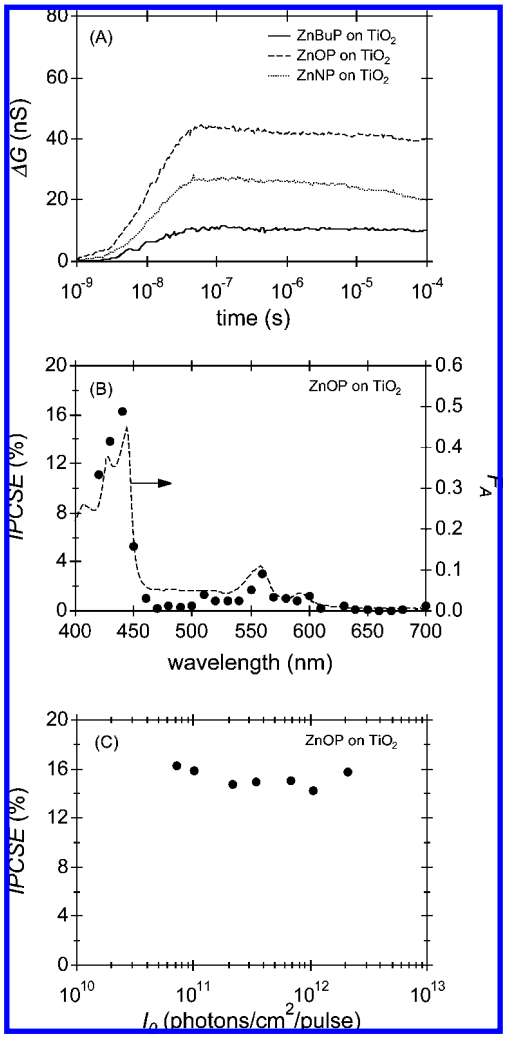

Figure 5. Photoconductance transients obtained on pulsed excitation (at 430 nm for ZnBuP, at 440 nm for ZnOP and ZnNP, with 10^{12} photons/cm^2/pulse) of the porphyrin derivatives on TiO_2 (A) and the *IPCSE* and fraction of absorbed light (F_A) as a function of wavelength for ZnOP on TiO_2 (B). Part (C) shows the *IPCSE* as a function of illumination intensity.

previously.[63] The *IPCSE* depends on the fraction of incident photons that is reflected by the bilayer (F_R), the number of excitons that reaches the porphyrin/TiO_2 interface normalized to the number of incident photons (S), and the interfacial electron injection yield relative to all modes of interfacial exciton deactivation (ϕ_{inj}) according to

$$IPCSE = (1 - F_R) \cdot S(\alpha, L, \Lambda_E) \cdot \phi_{inj} \cdot 100\% \qquad (4)$$

The factor S depends on the exponential absorption coefficient (α), the porphyrin layer thickness (L), and Λ_E. Analytical equations for S on back-side (S_{BR}, from the side of the TiO_2 substrate) and front-side (S_{FR}, from the side of the porphyrin film) illumination can be derived by solving the classical diffusion equation for steady-state conditions and are given in Appendix A (see Supporting Information).[63−65]

Accurate values for both ϕ_{inj} and Λ_E can be obtained by varying the thickness of the porphyrin layer. In case $L < \Lambda_E$,

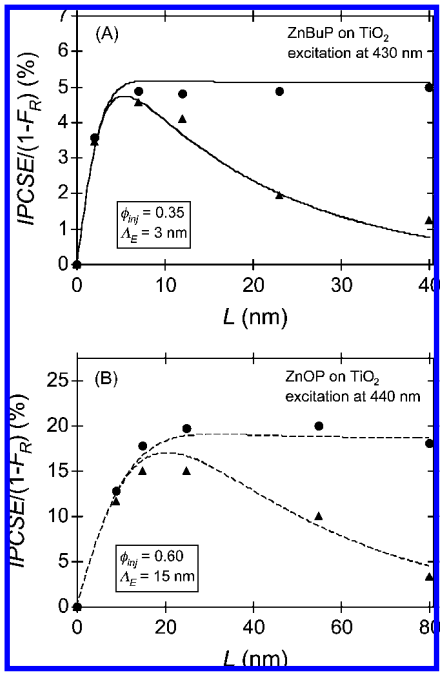

Figure 6. *IPCSE*/(1 − F_R) as a function of the porphyrin layer thickness (L) for ZnBuP on TiO_2 (A) and ZnOP on TiO_2 (B). Dots represent back-side illumination, and triangles, front-side illumination. The curves through the data points represent the fits of eqs 4, A3, and A4 to the experimental data; fit parameters are shown in the insets.

almost all excitons formed are able to reach the exciton-dissociating interface. Since the number of excitons formed is insensitive to the side of illumination, the *IPCSE* values on back-side and front-side illumination are expected to be comparable. Increasing L to values less than Λ_E leads to an increase of the *IPCSE*, both for back-side and for front-side illumination, since more light is absorbed as the porphyrin layer becomes thicker. In the case of backside illumination, a further increase of L does not result in an additional increase of the *IPCSE*, because mainly those excitons formed within a distance Λ_E from the interface can undergo interfacial charge separation. On the contrary, on front-side illumination increasing L results in a lower concentration of excitons near the porphyrin/TiO_2 interface. As a consequence the *IPCSE* decreases with increasing L and eventually becomes zero.

Figure 6 shows the *IPCSE* divided by (1 − F_R) as a function of L on back-side and front-side illumination for ZnBuP on TiO_2 (A) and ZnOP on TiO_2 (B). The reason for presenting the *IPCSE* divided by (1 − F_R) involves the difference in F_R between various samples. The experimental data presented in Figure 6 exhibit a layer thickness dependence that agrees with the expectations discussed above. Fitting eqs 4, A3, and A4 (see Appendix A of the Supporting Information) to the experimental data obtained for ZnBuP on TiO_2 results in $\Lambda_E = 3 \pm 1$ nm[66] and $\phi_{inj} = 0.35 \pm 0.05$. Combining an exciton diffusion length of 3 nm with an exciton lifetime of 74 ps yields an exciton diffusion coefficient of 1×10^{-7} m^2/s, as follows from eq 2. Assuming a center-to-center distance R_{DA} between ZnBuP molecules of 15 Å (diameter of a ZnBuP molecule) and using eq 1 yield an energy transfer rate equal to 4×10^{10} s^{-1}. Within

(63) Kroeze, J. E.; Savenije, T. J.; Vermeulen, M. J. W.; Warman, J. M. *J. Phys. Chem. B* **2003**, *107* (31), 7696−7705.
(64) Simpson, O. *Proc. R. Soc. London, Ser. A* **1957**, *238*, 402−411.
(65) Södergren, S.; Hagfeldt, A.; Olsson, J.; Lindquist, S. E. *J. Phys. Chem.* **1994**, *98* (21), 5552−5556.

(66) Note, that the root-mean-square diffusion distance (δ_D) is related to δ_E by $\delta_D = \sqrt{(2\delta)} \cdot \delta_E$ with δ as the dimensionality. The one-dimensional δ_D, in the direction perpendicular to the TiO_2 substrate, hence equals $\sqrt{2} \cdot \delta_E$.

Table 1. Parameters Characterizing the Energy Transfer in Isotropic ZnBuP Films, in Self-Assembled ZnOP Films, and in Natural Chlorosomes

light-harvesting system	Λ_E (nm)	τ_E (ps)	D_E (m^2/s)	R_{DA} (Å)	k_{ET} (ps^{-1})	τ_{ET} (ps)	$\tau_E \cdot k_{ET}$
ZnBuP	3	74	1×10^{-7}	15	0.04	23	3
ZnOP	15	160	1.4×10^{-6}	14.01	0.72	1.4	10^2
chlorosome	~15	~50[19]	5×10^{-6}	6.8[22]	10	0.1[19−21]	5×10^2

its lifetime of 74 ps an exciton can hop on average only 3 times between adjacent ZnBuP molecules.

The significantly larger ΔG and higher *IPCSE* observed for ZnOP and ZnNP on TiO_2 are indicative for more efficient exciton transport through films that consist of self-assembled stacks. The relatively poor solubility of ZnNP in toluene, however, does not allow preparing films thicker than 20 nm. The *IPCSE* divided by $(1 - F_R)$ as a function of L on back-side and front-side illumination is therefore only determined for ZnOP on TiO_2. Fitting eqs 4, A3, and A4 to the experimental data shown in Figure 6B results in $\Lambda_E = 15 \pm 1$ nm[66] and $\phi_{inj} = 0.60 \pm 0.05$. Combining an exciton diffusion length of 15 nm with an exciton lifetime of 160 ps gives an exciton diffusion coefficient equal to 1.4×10^{-6} m^2/s. Since the self-assembled stacks are aligned with their propagation direction parallel to the substrate, exciton motion in a direction perpendicular to the TiO_2 substrate occurs by interstack rather than by intrastack energy transfer, as shown schematically in Figure 4. The value of R_{DA} between an exciton-donating and -accepting ZnOP molecule is therefore taken equal to the interstack distance of 14.01 Å, determined by X-ray diffraction. Using eq 1, this distance and the found exciton diffusion coefficient yield $k_{ET} = 7.2 \times 10^{11}$ s^{-1}. Within its lifetime of 160 ps an exciton can on average make 10^2 hops before decay to the ground state occurs.

Origin of the Enhanced Exciton Diffusion Length. Table 1 summarizes the parameters involved in energy transfer in films of the porphyrin derivatives investigated, together with literature values for natural chlorosomes. Comparison of the energy transfer parameters for ZnBuP and ZnOP shows that self-assembly of the latter strongly enhances the exciton diffusion length. This is due to a longer exciton lifetime and a larger exciton diffusion coefficient, originating from a higher energy transfer rate, as discussed below. The exciton diffusion length in the self-assembled ZnOP film is comparable to that in natural chlorosomes. It can be seen in Table 1 that k_{ET} within a chlorosomal bacteriochlorophyll stack is more than 1 order of magnitude higher than that for ZnOP, as expected on the basis of the larger transition dipole moment of the Q-band of bacteriochlorophyll molecules. However, the larger value for R_{DA} and τ_E for ZnOP lead to a value for Λ_E comparable to that for a bacteriochlorophyll stack. In addition, it should be noted that the value for Λ_E determined for ZnOP corresponds to interstack exciton diffusion, while the Λ_E value for bacteriochlorophyll stacks refers to intrastack motion.

In the limit of weak intermolecular excitonic coupling, the motion of excitons can be considered as diffusive with an intermolecular hopping rate k_{ET} given by[67,68]

$$k_{ET} = \frac{2\pi}{\hbar}|V_{DA}|^2 J_{\mathrm{DA}} \qquad (5)$$

The factor V_{DA} denotes the excitonic coupling between the energy donor and acceptor, and J_{DA} represents the spectral overlap integral. The definition and evaluation of the spectral overlap integrals for ZnBuP and ZnOP are specified in Appendix B (see Supporting Information). The experimental absorption and fluorescence spectra yield comparable values for J_{DA} equal to 1.5×10^{18} J^{-1} for ZnBuP and 1.8×10^{18} J^{-1} for ZnOP. Hence, the much higher k_{ET} found for ZnOP is mainly due to a larger value of V_{DA}. Using eq 5 with the experimentally determined values for k_{ET} and J_{DA} yields excitonic couplings V_{DA} of 36 cm^{-1} for ZnBuP and 1.3×10^2 cm^{-1} for ZnOP. The value of V_{DA} equal to 1.3×10^2 cm^{-1} observed for ZnOP indicates a strong excitonic coupling between adjacent self-assembled stacks, which must originate from a favorable mutual orientation of molecules in adjacent stacks. Quantum-chemical calculations on excitonic couplings are underway in order to establish to which extent the value for interstack excitonic coupling can be understood on the basis of the molecular organizations deduced above and whether exciton transfer can be further improved.

Conclusions

This work involves a study of the relationship between molecular self-assembly of porphyrin derivatives and the ability to transport excitons efficiently to an active interface. ZnBuP films are found to have a disordered structure, in which the exciton diffusion length equals 3 ± 1 nm. In contrast, ZnOP molecules self-assemble via coordinative bonds between adjacent molecules. This leads to the formation of molecular stacks aligned parallel to a TiO_2 substrate. The diffusion length for exciton transport between the stacks is as long as 15 ± 1 nm. The large exciton diffusion length originates from both a long exciton lifetime and a strong excitonic coupling for interstack energy transfer. The difference in exciton diffusion length between ZnBuP and ZnOP demonstrates the importance of molecular self-assembly leading to efficient interstack exciton transport. The efficient interstack energy transfer has promising prospects for application of such self-assembled porphyrins in optoelectronics.

Acknowledgment. The authors thank Prof. Stephen J. Picken and Arkadiusz Kotlewski from the Nanostructured Materials Section of TU Delft for helpful discussions and assistance with polarized optical microscopy experiments, respectively. Marjan Versluijs from the Group of Inorganic Chemistry and Catalysis of Utrecht University is acknowledged for performing the XRD measurements. Research in Delft was supported financially by the Delft Research Centre for Sustainable Energy. B.M.J.M.S. and R.J.M.K.G. thank the Dutch Organization for Scientific Research NWO for a "Jonge Chemici" scholarship.

Supporting Information Available: A derivation of the analytical expressions for S on back-side and front-side illumination and definition and evaluation of spectral overlap integrals. This material is available free of charge via the Internet at http://pubs.acs.org.

JA075162A

(67) Pope, M.; Svenberg, C. E. *Electronic Processes in Organic Crystals and Polymers*, 2nd ed.; Oxford Science Publications: New York, 1999.
(68) Hennebicq, E.; Pourtois, G.; Scholes, G. D.; Herz, L. M.; Russell, D. M.; Silva, C.; Setayesh, S.; Grimsdale, A. C.; Mullen, K.; Bredas, J. L.; Beljonne, D. *J. Am. Chem. Soc.* **2005**, *127* (13), 4744−4762.